








ORIGINAL ARTICLE

Decreased expression of T-cell-associated immune markers predicts poor prognosis in patients with follicular lymphoma

Shinya Rai¹  | Hiroaki Inoue¹ | Kazuko Sakai²  | Hitoshi Hanamoto³ | Mitsuhiro Matsuda⁴  | Yasuhiro Maeda⁵ | Takahiro Haeno¹ | Yosaku Watatani¹ | Takahiro Kumode¹ | Kentaro Serizawa¹ | Yasuhiro Taniguchi¹  | Chikara Hirase¹ | J. Luis Espinoza¹  | Yasuyoshi Morita¹ | Hirokazu Tanaka¹ | Takashi Ashida¹ | Yoichi Tatsumi¹ | Kazuto Nishio²  | Itaru Matsumura¹ 

¹Department of Hematology and Rheumatology, Faculty of Medicine, Kindai University, Osaka-sayama, Japan

²Department of Genome Biology, Faculty of Medicine, Kindai University, Osaka-sayama, Japan

³Department of Hematology, Faculty of Medicine, Nara Hospital Kindai University, Ikoma, Japan

⁴Department of Hematology, PL General Hospital, Tondabayashi, Japan

⁵Department of Hematology, Minami Sakai Hospital, Sakai, Japan

Correspondence

Shinya Rai, Department of Hematology and Rheumatology, Faculty of Medicine, Kindai University, 377-2 Ohno-higashi, Osaka-sayama, Osaka 589-8511, Japan.
Email: rai@med.kindai.ac.jp

Abstract

We previously examined the utility of rituximab-bendamustine (RB) in patients with follicular lymphoma (FL) exhibiting less than optimal responses to 2 cycles of the R-CHOP chemotherapy regimen. The aim of this study was to identify molecular biomarkers that can predict prognosis in RB-treated patients in the context of the prospective cohort. We first analyzed the mutational status of 410 genes in diagnostic tumor specimens by target capture and Sanger sequencing. *CREBBP*, *KMT2D*, *MEF2B*, *BCL2*, *EZH2*, and *CARD11* were recurrently mutated as reported before, however none was predictive for progression-free survival (PFS) in the RB-treated patients ($n = 34$). A gene expression analysis by nCounter including 800 genes associated with carcinogenesis and/or the immune response showed that expression levels of CD8⁺ T-cell markers and half of the genes regulating Th1 and Th2 responses were significantly lower in progression of disease within the 24-mo (POD24) group ($n = 8$) than in the no POD24 group ($n = 31$). Collectively, we selected 10 genes (*TBX21*, *CXCR3*, *CCR4*, *CD8A*, *CD8B*, *GZMM*, *FLT3LG*, *CD3E*, *EOMES*, *GZMK*), and generated an immune infiltration score (IIS) for predicting PFS using principal component analysis, which dichotomized the RB-treated patients into immune IIS^{high} ($n = 19$) and IIS^{low} ($n = 20$) groups. The 3-y PFS rate was significantly lower in the IIS^{low} group than in the IIS^{high} group (50.0% [95% CI: 27.1–69.2%] vs. 84.2% [95% CI: 58.7–94.6%], $P = .0237$). Furthermore, the IIS was correlated with absolute lymphocyte counts at diagnosis ($r = 0.460$, $P = .00355$). These results suggest that the T-cell-associated immune markers could be useful to predict prognosis in RB-treated FL patients. (UMIN:000 013 795, jRCT:051 180 181)

Abbreviations: ALCs, absolute lymphocyte counts; B, bendamustine; CR, complete response; Cru, complete response unconfirmed; CTLs, cytotoxic T cells; FDCs, follicular dendritic cells; FFPE, formalin-fixed paraffin-embedded; FL, follicular lymphoma; FLIPI, Follicular lymphoma International Prognostic Index; G, obinutuzumab; GELF, Groupe d'Etude des Lymphomes Folliculaires; GEP, gene expression profiling; HR, hazard ratio; IIS, immune infiltration score; infil^{high}, immune infiltration^{high}; infil^{low}, immune infiltration^{low}; OS, overall survival; PFS, progression-free survival; POD24, progression of disease within 24 mo; R, rituximab; RB, rituximab-bendamustine; ROC, receiver operating characteristic; SNVs, single nucleotide variants; TAMs, tumor-associated macrophages; Tfh, T follicular helper; TME, tumor microenvironment; Treg, regulatory T.

This is an open access article under the terms of the Creative Commons Attribution-NonCommercial License, which permits use, distribution and reproduction in any medium, provided the original work is properly cited and is not used for commercial purposes.

© 2021 The Authors. *Cancer Science* published by John Wiley & Sons Australia, Ltd on behalf of Japanese Cancer Association.

KEYWORDS

bendamustine, follicular lymphoma, lymphopenia, POD24, tumor microenvironment

1 | INTRODUCTION

Follicular lymphoma is the most common indolent subtype of B-cell non-Hodgkin lymphomas.¹ The majority of FL patients present with advanced stages,¹ and those with high tumor burden and/or disease-related symptoms require immunochemotherapy.

To date, several chemotherapy regimens, including CHOP (cyclophosphamide, doxorubicin, vincristine, and prednisone), CVP (cyclophosphamide, vincristine, and prednisone), and bendamustine (B) in combination with anti-CD20 monoclonal antibodies such as rituximab (R) or obinutuzumab (G)^{2,3} have been recommended as front-line therapies in several guidelines.⁴⁻⁸ Most of the FL patients receiving these front-line immunochemotherapy regimens can obtain long-term survival benefit.⁹ However, c. 10%-20% of the patients experience progression of disease within 24 mo of diagnosis or treatment initiation (which is called POD24), and these patients have a substantially increased risk of death within 5 y after diagnosis.⁹⁻¹²

Given the heterogeneity of disease courses, several clinical risk stratification models, including FLIPI-1 and FLIPI-2, PRIMA-PI, and FLEX were proposed to predict the clinical outcomes of FL patients such as PFS and OS.¹³⁻¹⁶ However, most of these models have limited value to predict POD24. In addition, accumulated findings from genetic and GEP analyses showed that several molecular risk models mainly based on the intrinsic tumor properties, such as m7-FLIPI,¹⁷ POD24-PI¹⁸ and 23-GEP score,^{19,20} were useful tools to identify FL patients at high or low risk of progression after treatment with immunochemotherapy. In addition, a gene expression signature based on the extrinsic tumor environment, particularly focusing on the TME of FL, was established to predict POD24.¹¹ However, most of these models were mainly based on the data from the patients who received R-CHOP or R-CVP, and few reports are available to predict the prognosis of FL patients receiving B-based regimens.

We previously conducted a multicenter prospective phase 2 (CONVERT) trial, and demonstrated the utility of RB in patients with advanced FL exhibiting less than optimal responses to the initial 2 cycles of R-CHOP therapy.²¹ In addition, we reported that peripheral lymphopenia (<869/ μ L) before treatment was an independent poor prognostic factor for RB-treated FL patients in both our trial and validation cohorts.²¹ The main object of this study was to identify molecular biomarker(s) that could predict outcomes of the RB-treated FL patients in the context of the prospective cohort by genetic and GEP analyses.

2 | MATERIALS AND METHODS

2.1 | Study design and patients

The design and characteristics of the registered patients in the CONVERT trial have been described previously.²¹ All patients initially

received 2 cycles of standard R-CHOP. Patients who achieved CR/CR unconfirmed (CRu) according to Cheson's morphological criteria 1999²² (defined as an optimal response [OR] group) further received 4-6 cycles of R-CHOP treatment. The remaining patients who failed to achieve CR/CRu (defined as a non-OR [nOR] group), subsequently received 6 cycles of RB (R 375 mg/m² d1, B 90 mg/m² d1-2) every 28 d.

This study was designed and conducted according to the Declaration of Helsinki and was registered in UMIN (000 013 795) and jRCT (051 180 181). All patients provided written informed consent. The protocol, informed consent forms, and any amendments were approved by the institutional review boards of each hospital and certified review board.

2.2 | Target capture sequencing assay

DNA was extracted from FFPE samples using a DNA storm kit (Cell Data Sciences, Inc). The targeted DNA library for panel sequencing that was comprised of c. 1.65 Mb coding regions of all exons in 409 genes (Table S1) was constructed using an OncoPrint Tumor Mutation Load Assay (Thermo Fisher Scientific) according to the manufacturer's protocol. The purified libraries were pooled and then sequenced with an Ion Torrent S5 instrument and Ion 550 Chip Kit (Thermo Fisher Scientific). DNA sequencing data were accessed through the Torrent Suite v.5.10 program (Thermo Fisher Scientific). Reads were aligned against the hg19 human reference genome, and variants were analyzed with the use of Ion reporter v.5.10 (Thermo Fisher Scientific). Raw variant calls were manually checked using the Integrative Genomics Viewer (IGV; Broad Institute, MA). In this analysis, we defined the following criteria for the sequence quality: (1) the uniformity of amplicon coverage of >60%, and (2) the minimum quality criterion was 80% of target bases with $\geq 100\times$ sequencing coverage. The mutations were filtered with the exclusion of: (1) Fisher exact test, P -value $> 10^{-4}$, (2) Phred QUAL score of <99, and (3) allele frequency in tumor <0.025, and missense SNVs with an allele frequency of 0.45-0.55 in copy-neutral regions, unless they were listed in the COSMIC database (v.70) or reported to be mutated in FL. Germline mutations were excluded using the NCBI dbSNP build 131 and UCSC genome browser database.^{23,24}

2.3 | Sanger sequencing analysis

Exons 2 and 3 of *MEF2B* were analyzed using the PCR primers designed with Primer3 software. The *MEF2B* coding exons 2 and 3 were amplified using PCR. After visual confirmation of amplification, the PCR product was submitted for Sanger sequence analysis

as previously described.²⁵ The sequences of the PCR primers used in this study are shown in Table S2.

2.4 | The m7-FLIPI score calculation

The m7-FLIPI score was calculated using the calculator presented at the German Low-Grade Lymphoma Study Group official internet site (www.gls.de/m7-flipi/). The same cut-off level as used in the original publication was applied to determine high-risk and low-risk categories (m7-FLIPI scores ≥ 0.8 and < 0.8 , respectively).¹⁷

2.5 | Gene expression profiling analysis

RNA was extracted from FFPE samples using an RNA storm kit (Cell Data Sciences, Inc). Details of the nCounter assay (NanoString Technologies, Seattle, WA, USA) have been reported previously.^{24,26} In this study, a customized pan-cancer immune-profiling panel (NanoString Technologies), which consists of 770 genes related to cancer or immune cells and an additional 30 genes (Table S3), was used for nCounter-based gene expression measurements. The data were analyzed using nSolver 4.0 software (NanoString) and JMP version 13.0 software (SAS Institute).

2.6 | Immune infiltration score calculation

To generate an IIS for predicting PFS, we performed a principal component analysis, which used orthogonal rotation to extract the components whose eigenvalues were greater than 1.0 (SPSS statistics v.24.0). Subsequently, a multivariate Cox proportional hazards analysis for PFS was performed with the extracted components as explanatory variables. Finally, the IIS was calculated as the sum of the score matrix of each gene. Expression levels from selected genes were multiplied by z-score. ROC analyses were performed to determine the optimal cut-off values of the IIS to predict PFS by the Youden index calculation algorithm. The formula of the IIS was as followed: $(CD8A \times 0.161 + CD3E \times 0.160 + CD8B \times 0.157 + EOMES \times 0.157 + GZMK \times 0.153 + CXCR3 \times 0.139 + GZMM \times 0.132 + FLT3LG \times 0.121 + TBX21 \times 0.075 + CCR4 \times 0.072)$.

2.7 | Statistical analysis

The cut-off date for this analysis was December 31, 2019. The survival analysis was performed using a Kaplan-Meier method, which was evaluated by log-rank test. Fisher exact test and Benjamini-Hochberg correction for multiple testing were used for between-category data comparisons. For the comparison of 2 continuous variables, data were tested by Wilcoxon rank sum test. Spearman correlation coefficients were estimated as continuous variables. Statistical analyses were performed with R 4.1.0 software (The R

Foundation for Statistical Computing), and a P -value $< .05$ was considered statistically significant.

3 | RESULTS

3.1 | Patient characteristics and clinical outcomes

In total, 56 patients initially received 2 cycles of R-CHOP. Then, 13 patients (23.2%), who achieved CR/CRu (OR group), continued R-CHOP for further 4-6 cycles. The remaining 43 patients (76.8%), who were judged as nOR, received RB as the protocol treatment. The FFPE samples were available for extraction of DNA and/or RNA in 50/56 cases (89.3%, [OR $n = 10$, nOR $n = 40$]) for this study. The baseline characteristics of these 50 cases are shown in Table 1. The median treatment cycle of RB in the nOR group ($n = 40$) was 6 cycles (range, 2-6), and 30/40 cases (75.0%) completed 6 cycles of RB. At a median follow-up time of 47.4 mo (range: 3.20-79.3), the PFS and OS rates at 3 y in all cases ($n = 50$) were 71.0% (95% CI: 56.0%-81.7%) and 93.5% (95% CI: 81.2%-97.9%), respectively (Figure S1A, B). The 3-y PFS rates were 87.5% in the OR group (95% CI: 38.7%-98.1%) and 67.5% in the nOR group (95% CI: 50.7%-9.7%), respectively, with no statistically significant difference ($P = .213$).

We next investigated whether FLIPI could be applied in the nOR group ($n = 40$). The proportions of patients in the low-, intermediate-, and high-risk groups by FLIPI were 5.0% (2/40) and 37.5% (15/40), and 57.5% (23/40), respectively (Table 1). The high-risk group tended to have an inferior 3-y PFS rate (60.9%, [95% CI: 38.3%-77.4%]) compared with the low-risk group (100% [95% CI: NA]) and the intermediate-risk group (73.3%, [95% CI: 43.6%-89.1%]), but without a statistically significant difference ($P = .323$) (Figure S1C).

3.2 | Mutational landscape of the whole population

To investigate the mutational landscape in this cohort, we performed the target capture sequence using tumor samples from the above-described 50 cases. Eight cases (OR $n = 2$, nOR $n = 6$) were excluded from this analysis because of their poor DNA qualities. Therefore, 42 cases (OR $n = 8$, nOR $n = 34$) were analyzed on the targeted panel for 409 genes, in which most of the recurrently mutated genes in FL were included except *MEF2B*. *MEF2B* encodes a transcriptional activator and is mutated in 10%-20% of FL and its mutational status is applied in m7-FLIPI.²⁷ Therefore, we analyzed its mutation status by Sanger sequencing independently. In this analysis, we focused on exon 2 and exon 3 of *MEF2B*, because most of *MEF2B* mutations in FL were scattered around these regions.²⁸ As a result, *MEF2B* mutations were identified in 13/42 cases (31.0%), all consisting of L67R in the exon 3, in which the mutated site was reported to play an important role in the interaction with EP300 proteins.²⁸ The double mutations with L67R and G2R in exon 2 were identified in 1 case (Figure 1A and Table S4).

TABLE 1 Patient characteristics

	All (n = 50)	OR (N = 10)	nOR (N = 40)	P-value
Age (y)				
Median [range]	62.5 [36.0, 78.0]	64.0 [54.0, 78.0]	65.0 [36.0, 76.0]	.622
Sex n(%)				
Female	29 (58.0)	6 (60.0)	23 (57.5)	1
Male	31 (42.0)	4 (40.0)	17 (42.5)	
Grade n (%)				
1	12 (24.0)	1 (10.0)	11 (29.7)	.532
2	23 (46.0)	6 (60.0)	17 (45.9)	
3a	12 (24.0)	3 (30.0)	9 (24.3)	
Stage n (%)				
II	3 (6.00)	0 (00.0)	3 (7.50)	.036
III	17 (34.0)	7 (70.0)	10 (25.0)	
IV	30 (60.0)	3 (30.0)	27 (67.5)	
B symptoms n (%)				
Bone marrow involvement n (%)	9 (18.0)	3 (30.0)	6 (18.2)	1
Bulky disease >7 cm n (%)	27 (54.0)	4 (30.8)	23 (57.5)	.164
	18 (36.0)	0 (0.00)	18 (45.0)	.009
GELF criteria				
Low	2 (4.00)	1 (10.0)	1 (2.50)	.363
FLIPI n (%)				
Low	3 (6.00)	1 (10.0)	2 (5.00)	.07
Intermediate	22 (44.0)	7 (70.0)	15 (37.5)	
High	25 (50.0)	2 (20.0)	23 (57.5)	
FLIPI-2 n (%)				
Low	0 (0.00)	0 (0.00)	0 (0.00)	.308
Intermediate	27 (54.0)	7 (70.0)	20 (50.0)	
High	23 (46.0)	3 (30.0)	20 (50.0)	

When the results from target capture sequencing and Sanger sequencing were combined, a total of 34 genes was found to be recurrently mutated (in ≥ 2 cases), including 107 non-synonymous SNVs, 19 multiple mutations, 16 frameshift insertions or deletions, 13 stop-gain mutations, and 7 non-frameshift insertions or deletions. Overall, 37/42 cases (88.1%) had at least 1 coding mutation within 410 genes with a median of 4 mutations per patient (range 0-10) (Figure 1A), and the average depth of sequencing coverage in the 37 cases was 882 \times (103-3999 \times). The most recurrently mutated genes were *CREBBP* (59.5%), *KMT2D* (38.1%), *MEF2B* (31.0%), *BCL2* (28.6%), *EZH2* (21.4%), *CARD11* (16.7%), *TNFRSF14*, and *EP300* (14.3% each), *APC* (11.9%), with the landscape closely resembling the previous reports^{1,29,30} (Figure 1B). Positions and types of somatic mutations in these genes are shown in Figure S2 and Table S4.

3.3 | Association of mutation profile with clinical outcomes in the nOR group

Among recurrently mutated genes, their mutation frequencies (in $\geq 10\%$) in the OR and nOR groups are shown in Table 2. Next, we

analyzed whether mutation status influenced the outcomes in the nOR group (n = 34). As shown in Figure 2A, the mutation status of the specific gene did not influence PFS significantly in univariate analyses. We also evaluated the influence of gene mutations on POD24; however, there were no statistically significant differences between the 2 groups (Figure 2B). Interestingly, no POD24 event occurred in RB-treated patients with *CARD11* mutations in the nOR group. In addition, the cases with *CARD11* mutations tended to have a better 3-y PFS rate than unmutated cases but with no statistically significant difference (100% vs. 59.3%, $P = .174$) (Figure 2C).

3.4 | Association of m7-FLIPI with clinical outcomes

We next investigated whether m7-FLIPI could be applied to this total cohort (n = 42). As expected, no cases (0/8) in the OR group were classified into the high-risk category in the m7-FLIPI compared with 29.4% (10/34) in the nOR group but without a significant difference ($P = .165$) (Table 2). The high-risk group tended to have an inferior 3-y PFS rate compared with the low-risk group (76.8% [95%

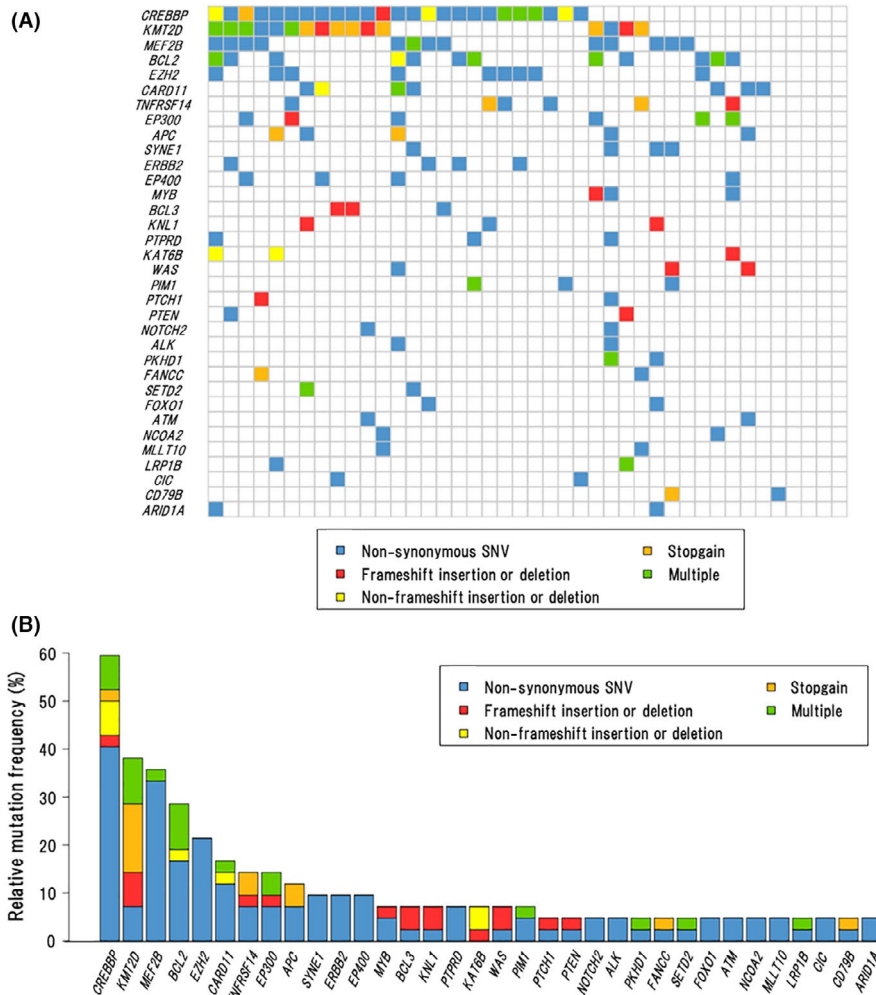


FIGURE 1 Landscape of somatic mutations. A, Co-mutation plot showing the spectrum of recurrently mutated genes across all cases ($n = 42$). B, Frequencies and types of somatic mutations in 34 recurrently mutated genes (found in ≥ 2 cases) for all cases ($n = 42$)

CI: 57.4%-88.2%] vs. 60.0% [95% CI: 25.3%-82.7%]) but without a significant difference ($P = .104$) (Figure 3A).

Next, we focused on RB-treated patients ($n = 34$) in the nOR group. In this group, the proportion of cases in the low- and high-risk categories in m7-FLIPI was 70.6% (24/34) and 29.4% (10/34), respectively (Table 2). At a median follow-up time of 48.7 mo (4.07-79.3), the 3-y PFS rates were 70.8% in the low-risk group (95% CI: 48.4%-84.9%) and 60.0% in the high-risk group (95% CI: 25.3%-82.7%), without a significant difference ($P = .264$) (Figure 3B). Among 24 cases in the low-risk group, 4 cases experienced POD24 (16.7%), while 3 from 10 cases in high-risk group experienced POD24 (30%) without a significant difference (OR: 0.467, [95%CI: 0.0830-2.62], $P = .394$) (Figure 3C).

3.5 | Association of the 23-gene expressions with clinical outcomes

We next analyzed gene expression levels using the FFPE samples from the above-described 50 patients. Two cases (OR $n = 1$, nOR $n = 1$) were excluded from this analysis because of their poor RNA qualities. Therefore, 48 cases (OR $n = 9$, nOR $n = 39$) were analyzed by the nCounter system. Sample quality was assessed by

mRNA levels of 40 housekeeping genes in each sample (Table S3). It has been previously reported that the GEP score based on the expression of 23 genes was associated with clinical outcomes of FL cases,¹⁹ which was confirmed by the following study.²⁰ Furthermore, the 23 genes could identify 2 main clusters characterized by high or low expression associated with favorable or poor outcomes.²⁰ So, we subjected our 48 cases to hierarchical clustering using these 23 genes. Consistent with the previous reports,^{19,20} we could identify 2 main clusters (cluster 1 and cluster 2) (Figure 4A), however, at a median follow-up time of 47.4 mo (3.2-79.3), 3-y PFS rates did not differ significantly between the 2 clusters (74.7% [95% CI: 55.6%-86.5%] vs. 60.0% [95% CI: 31.8%-79.7%], $P = .436$) (Figure 4B).

Next, we compared 3-y PFS rates between clusters 1 and 2 in the RB-treated 39 patients. At a median follow-up time of 46.1 mo (3.2-79.3), the patients in cluster 2 tended to have an inferior 3-y PFS rate compared with those in cluster 1 (50.0% [95% CI: 18.4%-75.3%] vs. 72.4% [95% CI: 52.3%-85.1%]) but without a significant difference ($P = .263$) (Figure 4C). We further compared the expression of 23 genes between 8 patients with POD24 and 31 patients without POD24. Although these genes were reported to portend good or poor risk, the expression levels of these genes were almost equivalent in the 2 groups (Figure S3).

TABLE 2 Mutation frequencies of recurrently mutated genes in all cases, OR group, and nOR group

Genes	Mutation presence	All (n = 42)	OR (N = 8)	nOR (N = 34)	P-value
APC n (%)	Absence	37 (88.1)	7 (87.5)	30 (88.2)	1
	Presence	5 (11.9)	1 (12.5)	4 (11.8)	
ARID1A n (%)	Absence	40 (95.2)	8 (100.0)	32 (94.1)	1
	Presence	2 (4.80)	0 (0.00)	2 (5.90)	
BCL2 n (%)	Absence	30 (71.4)	7 (87.5)	23 (67.6)	.402
	Presence	12 (28.6)	1 (12.5)	11 (32.4)	
CARD11 n (%)	Absence	35 (83.3)	8 (100.0)	27 (79.4)	.312
	Presence	7 (16.7)	0 (0.00)	7 (20.6)	
CREBBP n (%)	Absence	17 (40.5)	5 (62.5)	12 (35.3)	.235
	Presence	25 (59.5)	3 (37.5)	22 (64.7)	
EP300 n (%)	Absence	36 (85.7)	8 (100.0)	28 (82.4)	.576
	Presence	6 (14.3)	0 (0.00)	6 (17.6)	
EP400 n (%)	Absence	38 (90.5)	8 (100.0)	30 (88.2)	.572
	Presence	4 (9.50)	0 (0.00)	4 (11.8)	
ERBB2 n (%)	Absence	38 (90.5)	7 (87.5)	31 (91.2)	1
	Presence	4 (9.50)	1 (12.5)	3 (8.80)	
EZH2 n (%)	Absence	33 (78.6)	8 (100.0)	25 (73.5)	.168
	Presence	9 (21.4)	0 (0.00)	9 (26.5)	
FOXO1 n (%)	Absence	40 (95.2)	8 (100.0)	32 (94.1)	1
	Presence	2 (4.80)	0 (0.00)	2 (5.9)	
KMT2D n (%)	Absence	26 (61.9)	7 (87.5)	19 (55.9)	.127
	Presence	16 (38.1)	1 (12.5)	15 (44.1)	
MEF2B n (%)	Absence	29 (69.0)	5 (62.5)	24 (70.6)	.686
	Presence	13 (31.0)	3 (37.5)	10 (29.4)	
SYNE1 n (%)	Absence	38 (90.5)	7 (87.5)	31 (91.2)	1
	Presence	4 (9.50)	1 (12.5)	3 (8.80)	
TNFRSF14 n (%)	Absence	36 (85.7)	7 (87.5)	29 (85.3)	1
	Presence	6 (14.3)	1 (12.5)	5 (14.7)	
m7FLIPI n (%)	Low	32 (76.2)	8 (100.0)	24 (70.6)	.165
	High	10 (23.8)	0 (0.00)	10 (29.4)	

3.6 | Association of the T-cell-associated gene expression with clinical outcomes

In this trial, we previously reported that a low ALCs was an independent poor prognostic factor for RB-treated patients.²¹ Because lymphopenia was considered to reflect an immune-suppressive state, we applied a customized pan-cancer immune-profiling panel, which consisted of 800 genes related to cancer development and/or immune reactions, to the RB-treated case in the nOR group (n = 39). As a result, a total of 33 genes, including 2 upregulated (*CD79a* and *POU2F2*) and 31 downregulated genes (each with \log_2 fold change > |0.5|, and corrected $[-\log_{10}P] > 1.5$) were differentially expressed in the POD24 group (n = 8) compared with the no POD24 group (n = 31). Of interest, the top genes downregulated in the POD24 group were markedly enriched with T-cell-associated genes (Figure 5A).

Therefore, we further compared the expression levels of molecules specific for various types of T cells (Th1, Th2, and Th17, Tfh, Treg, natural killer (NK), and CD8⁺ T cells) and of immune checkpoint markers between the 2 groups. Interestingly, the expression levels of CD8⁺ T-cell marker genes (*CD8A*, *CD8B*, *FLT3LG*, *EOMES*, *GZMM*, *GZMK*) except for *PRF1* were significantly lower in the POD24 group compared with the no POD24 group (Figure 5B). Furthermore, about half of the genes related to Th1 and Th2 responses in T cells were downregulated in the POD24 group compared with those in the no POD24 group (Figure S4). Among them, expression levels of several genes that had been reported to regulate differentiation (*EOMES*,^{31,32} *TBX-21*³³) or migration (*CXCR3*^{34,35}) of CD8⁺ T cells were significantly lower in the POD24 group. Unexpectedly, *CCR4*, known to be mainly expressed on Treg cells, was downregulated in the POD24 group. In contrast, NK cell markers and immune checkpoint markers were

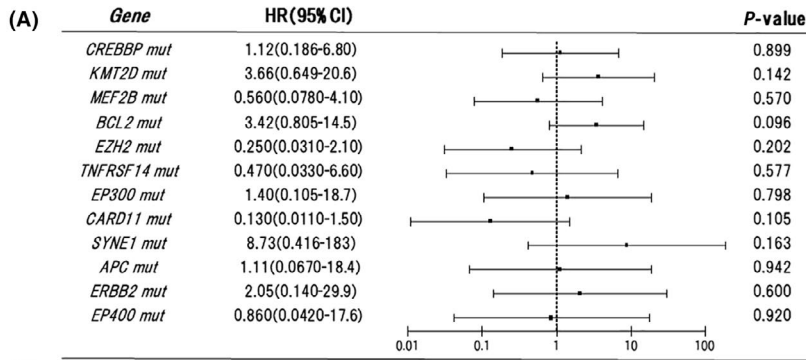


FIGURE 2 Association of mutation profile with clinical outcomes in the nOR group. A, Forest plot for progression-free survival in univariate analyses. HR, hazard ratio. Mut, mutations. B, Frequencies of mutations in 34 recurrently mutated genes in cases with or without POD24 in the nOR group (n = 34). C, Kaplan-Meier curves for progression-free survival of cases with or without *CARD11* mutations in the nOR group (n = 34). Log-rank P-values are shown in the graphs. Wt, wild type. Mut, mutations

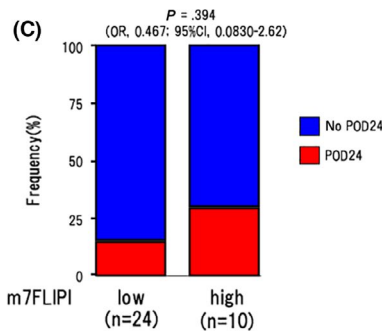
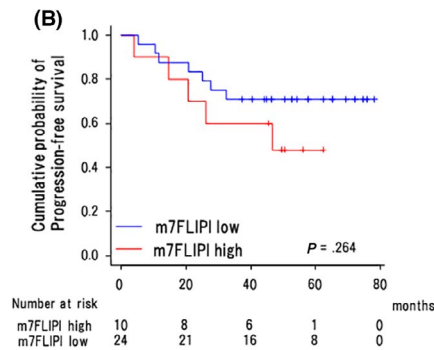
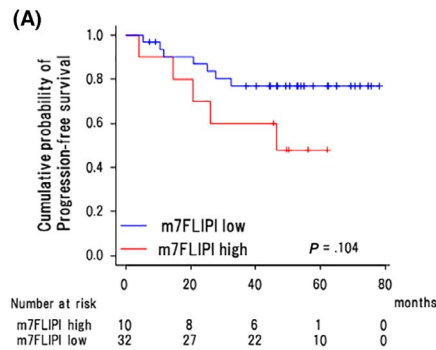
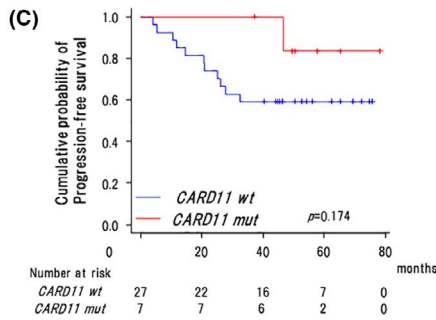
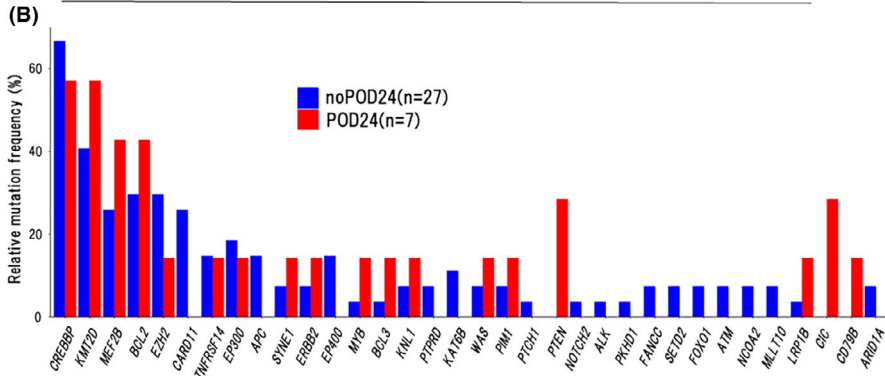


FIGURE 3 Association of m7-FLIPI with clinical outcomes. Comparison of progression-free survival between the cases in the low-risk and high-risk categories classified by m7-FLIPI for (A) all cases (n = 42) and (B) nOR group (n = 34). Log-rank P-values are shown in the graphs. Int, intermediate. C, The proportions of the low-risk and high-risk categories classified by m7-FLIPI in the cases with and without POD24 in the nOR group (n = 34). P-values by Fisher exact test are shown in the graphs

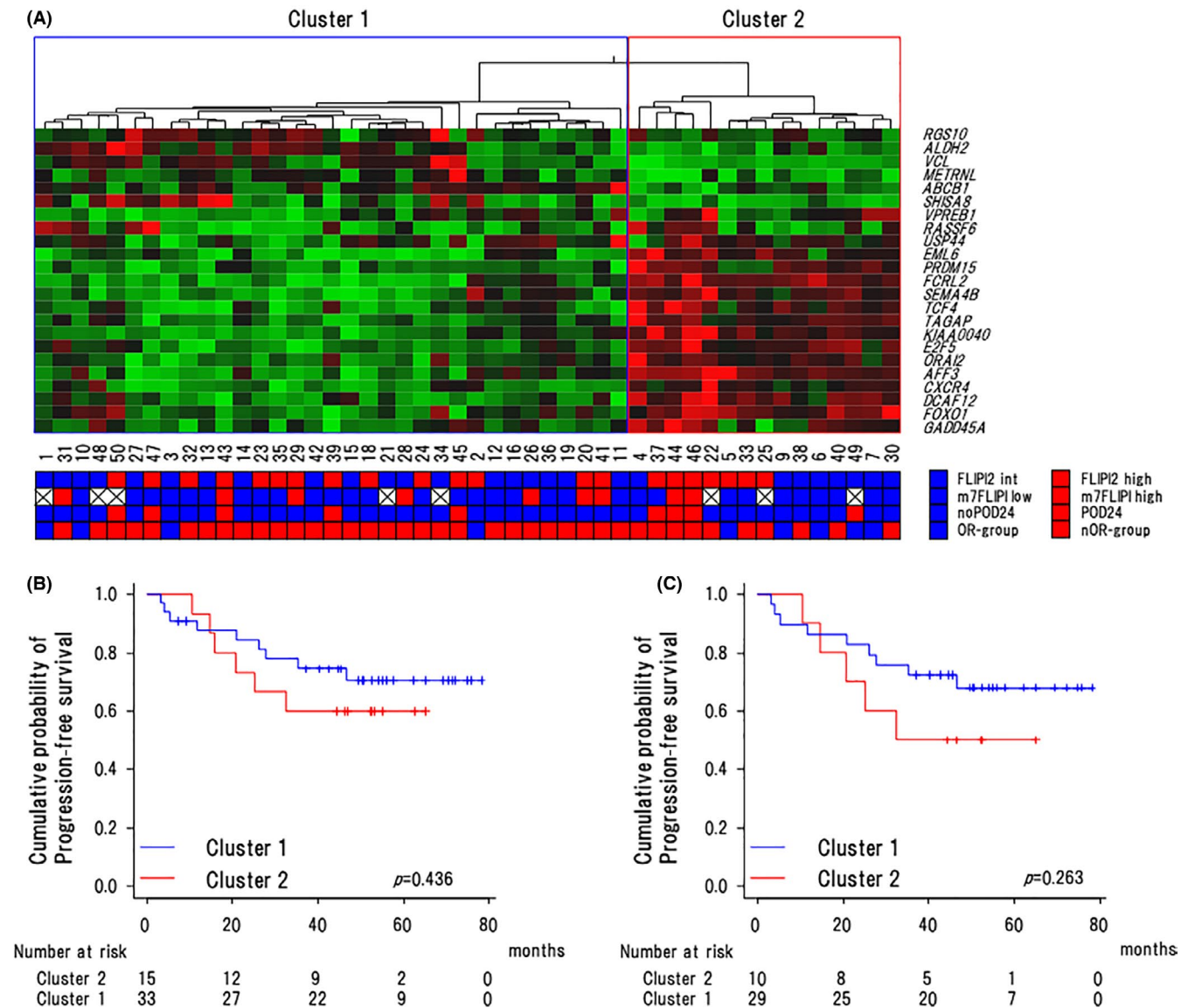


FIGURE 4 Association of the 23-gene expression levels with clinical outcomes. A, Heat map and unsupervised hierarchical clustering showing the genes along rows and cases along columns in all cases. Green denotes low and red indicates high gene expression. Clusters 1 and 2 were characterized by high expression of genes associated with favorable and poor outcome, respectively. B, Kaplan-Meier curves for progression-free survival of cases with clusters 1 and 2 in all cases ($n = 48$). C, the nOR group ($n = 39$). Log-rank P -values are shown in the graphs

almost equivalently expressed in the 2 groups (Figures 5B and S4). So, we speculated that the prognosis of the FL patients might be influenced by CD8⁺ T-cell infiltration.

3.7 | Association of the immune infiltration score with clinical outcomes

Next, we selected 10 genes (*TBX21*, *CXCR3*, *CCR4*, *CD8A*, *CD8B*, *GZMM*, *FLT3LG*, *CD3E*, *EOMES*, *GZMK*) by manual curation that are involved in differentiation and/or migration of CD8⁺ T cells and performed unsupervised hierarchical clustering. As a result, we could dichotomize 39 RB-treated cases into immune infiltration^{high}

(infil^{high}) and infiltration^{low} (infil^{low}) clusters (Figure 6A). Of note, POD24 was observed in 8/20 (40%) cases in the infil^{low} cluster, and no POD24 event occurred in the infil^{high} cluster with significant difference ($P = .0084$) (Figure 6B).

Next, we attempted to generate an IIS using these 10 genes. For this purpose, we conducted a principal component analysis on 39 cases in the nOR group and extracted 3 principal components (Table S5). Eventually, principal component 1 had a prognostic value for PFS (HR 0.382, 95% CI: 0.170-0.856, $P = .0194$; Table S6). So, we calculated the IIS using this component. The IIS ranged from -1.986 to 2.937 , and a score of -0.197 was determined as the optimum threshold to separate these cases into IIS^{low} ($n = 20$) and IIS^{high} ($n = 19$) groups from ROC analysis (specificity = 0.624,

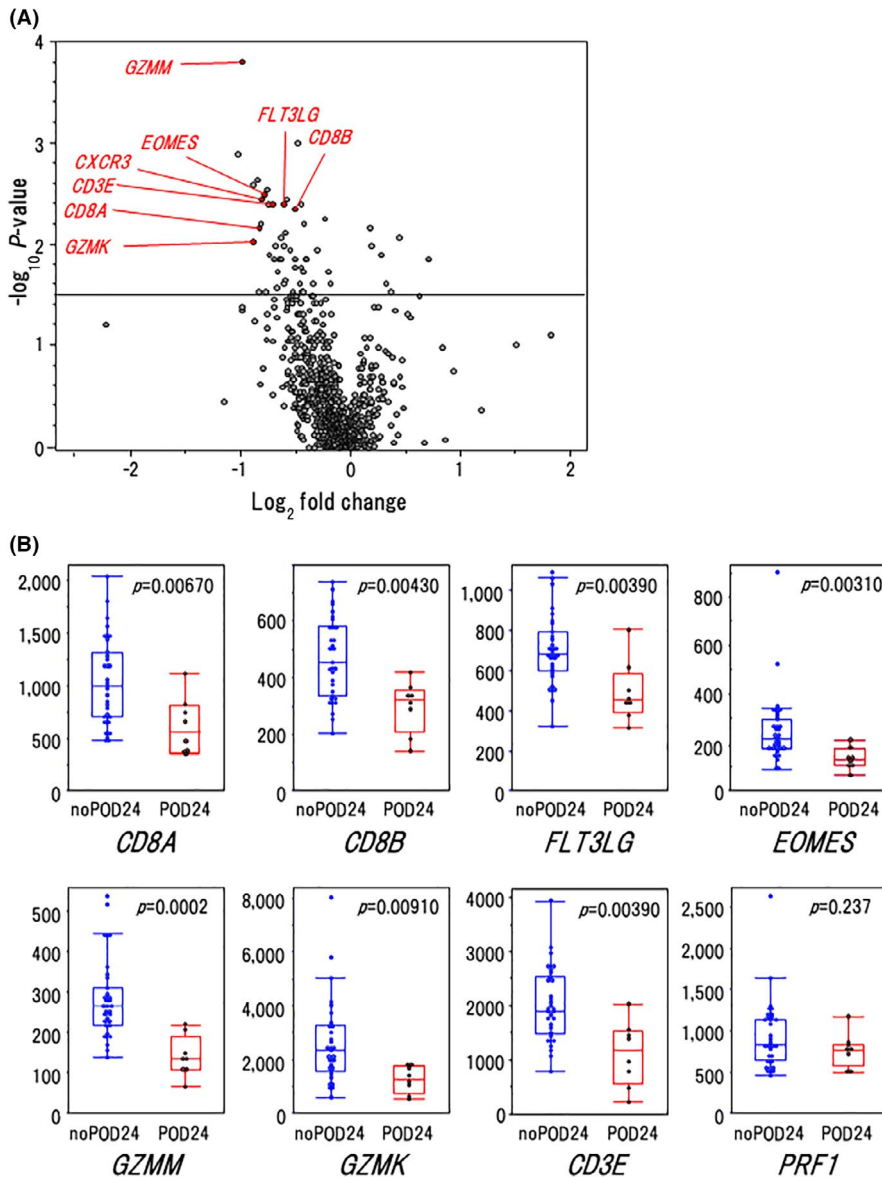


FIGURE 5 Association of T-cell-associated gene expression with clinical outcomes. A, Volcano plot indicating differentially expressed genes in cases with or without POD24 in the nOR group ($n = 39$). B, Gene expression levels of the $CD8^+$ T-cell markers in the cases with POD24 and without POD24. P -values by Fisher exact test are shown in the graphs. In the box plots, the center line and lower and upper hinges correspond to the median, and the first and third quartiles (25 and 75 percentiles), respectively. The upper and lower whiskers extend from the upper and lower hinges to the largest or smallest values no further than a $1.5 \times$ inter-quartile range from the hinges

sensitivity = 0.786, AUC = 0.719; Figure S5). The 3-y PFS rate was significantly lower in the IIS^{low} group compared with in the IIS^{high} group (50.0% [95% CI: 27.1%-69.2%] vs. 84.2% [95% CI: 58.7%-94.6%], $P = .0237$) (Figure 6C). We also examined the relationship between the IIS and ALCs in these 39 patients and found that the IIS was correlated with ALCs ($r = 0.460$, $P = .00355$; Figure 6D).

3.8 | Association of the T-cell-associated gene expression with their mutation profile

We next analyzed whether gene mutations influenced the expression of T-cell-associated genes in 40 patients. However, the frequencies of mutations were roughly the same between infil^{low} and infil^{high} clusters in most genes (Figure 7A). For example, the mutation frequencies in *CREBBP*,³⁶ *EZH2*,³⁷ and *TNFRSF14*,³⁸ which are known to regulate the tumor microenvironment, did not differ significantly between the 2 clusters.

Finally, we investigated whether the IIS was correlated with ALCs using all cases ($n = 48$) and found that the IIS was correlated with ALCs also in this population ($r = 0.349$, $P = .0156$; Figure 7B). Of note, the mean number of ALCs was significantly lower in the IIS^{low} group (1120/ μ L) than in the IIS^{high} group (1560/ μ L) ($P = .0198$) (Figure 7C). Furthermore, the proportion of cases with low ALCs (<869/ μ L) was higher in the IIS^{low} group than in the IIS^{high} group (41.7% vs. 8.33%, OR: 7.86 [95%CI, 1.49-41.3], $P = .0173$) (Figure 7D).

4 | DISCUSSION

In this study, we attempted to identify biomarker(s) that can predict clinical outcomes of RB-treated FL patients. At first, we examined gene mutation profiles in our patients. As a result, we found that types of mutated genes and their frequencies were roughly the same as previously reported,^{1,29,30} and we found that none of those mutations influenced PFS in univariate analyses. Among them, mutations

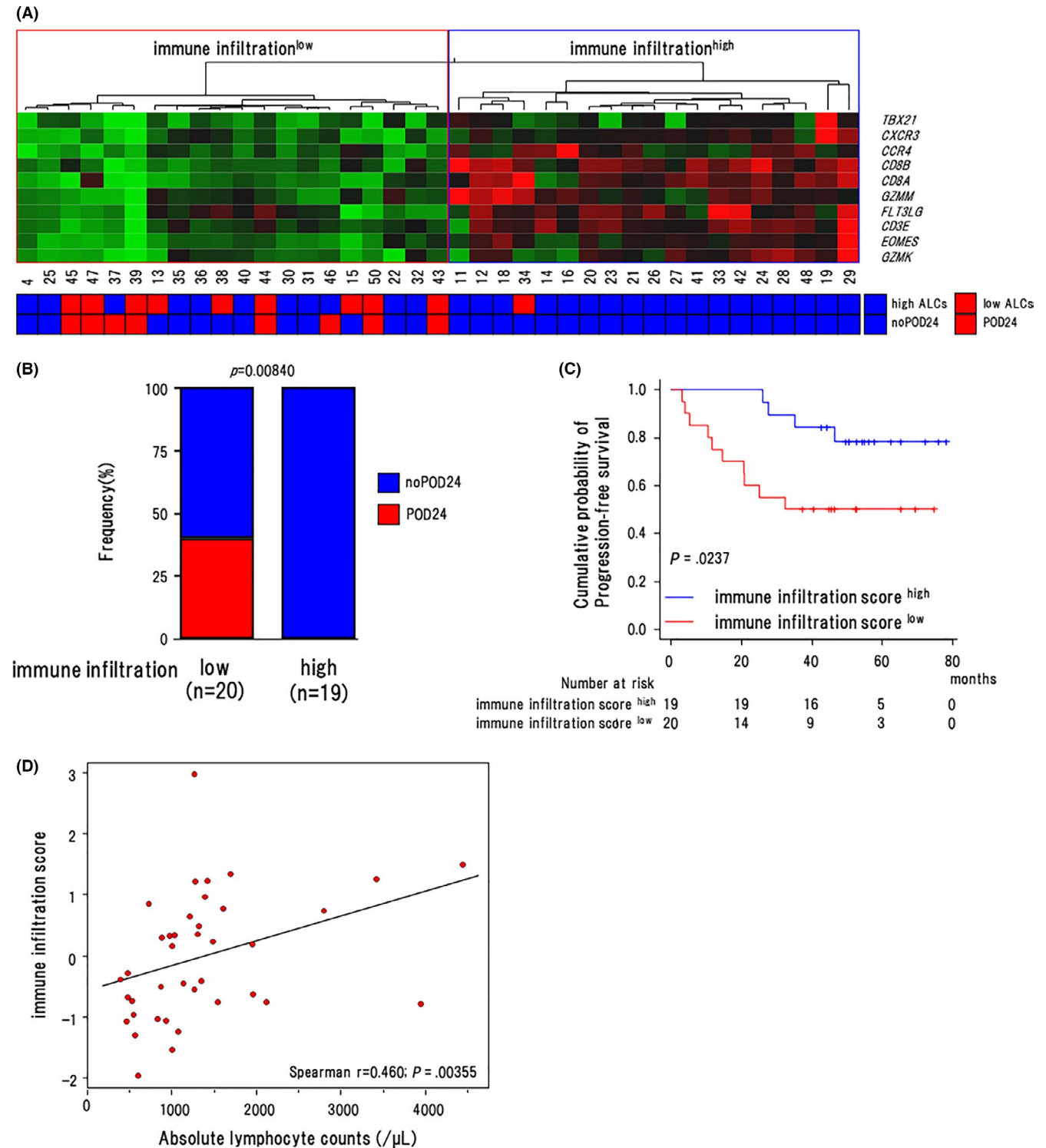


FIGURE 6 Association of the immune infiltration score with clinical outcomes. A, Heat map and unsupervised hierarchical clustering showing the genes along rows and cases along columns in the nOR group. Green denotes low and red indicates high gene expression. The regions indicate the low (shown in red) and high immune infiltration cluster (shown in blue). B, The proportion of cases with POD24 in the infil^{low} and infil^{high} clusters in the nOR group. P-values by Fisher exact test are shown in the graphs (n = 39). C, Progression-free survival of cases in the IIS^{low} (n = 20) and IIS^{high} (n = 19) groups in the nOR group (n = 39). Log-rank P-values are shown in the graphs. D, Scattergram shows the correlation between ALCs (horizontal axis) and IIS (vertical axis). Spearman's correlation coefficients are estimated as continuous variables

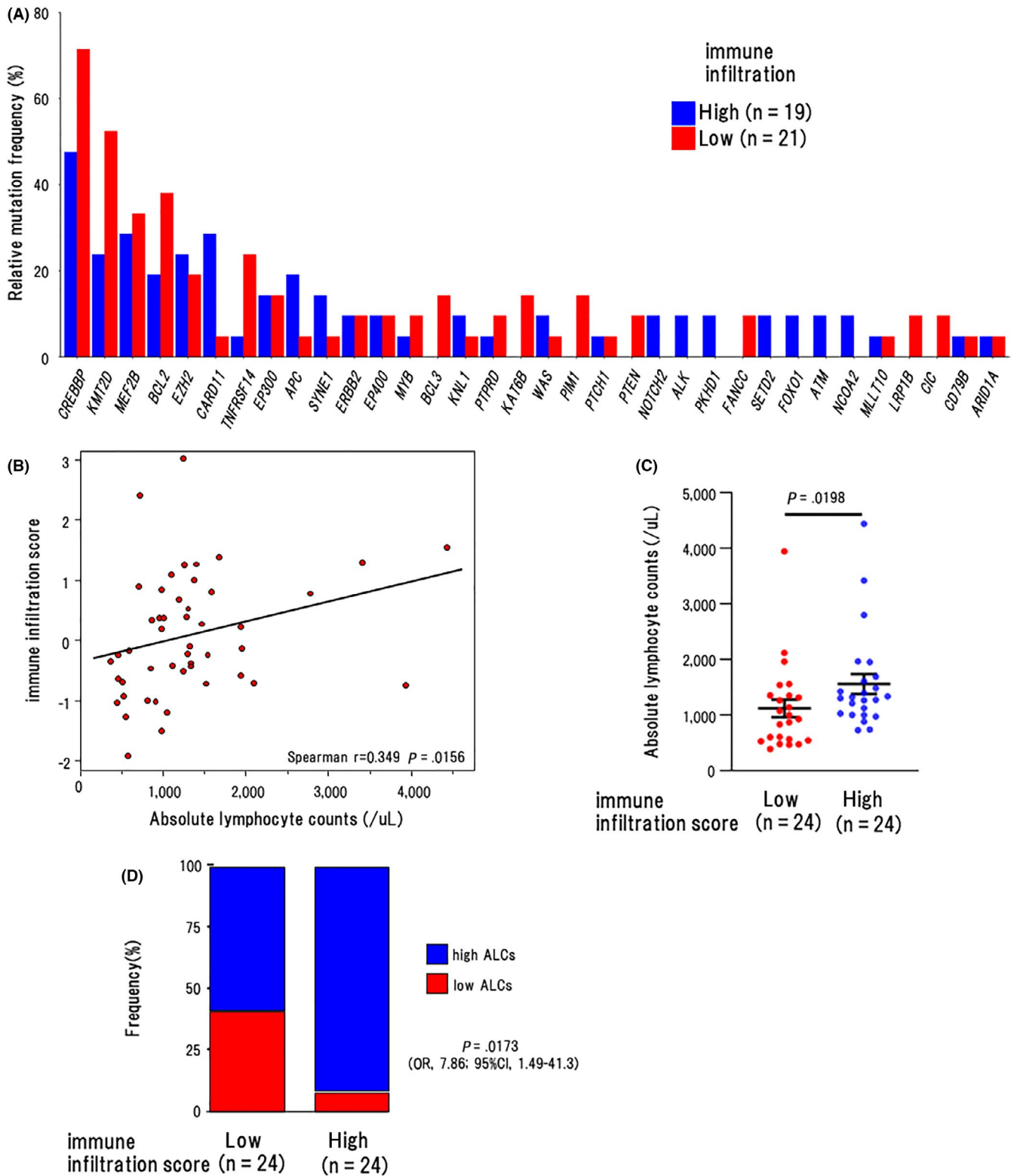


FIGURE 7 Association of the T-cell-associated gene expression with their mutation profile. A, Mutation frequencies of recurrently mutated genes by infil^{low} and infil^{high} clusters in all cases (n = 40). B, Scattergram shows the correlation between ALCs (horizontal axis) and IIS (vertical axis). Spearman correlation coefficients were estimated as continuous variables. C, The number of ALCs in the IIS^{low} (n = 24) and IIS^{high} (n = 24) groups. P -values using Wilcoxon rank sum test are shown in the graphs. The graph shows the mean and SEM of data from the cases in the respective groups. D, The proportion of cases with low ALCs (< 869/ μ L) in the IIS^{low} (n = 24) and IIS^{high} (n = 24) groups. P -values using Fisher exact test are shown in the graphs

of *CARD11*, which functions as a positive regulator of the NF- κ B pathway in normal B and T lymphocytes, were detected in 16.7% of the cases. A *CARD11* mutation was more frequently observed in transformed FL than in untransformed FL^{29,39} and counted as a poor prognostic factor in m7-FLIPI.¹⁷ In accordance with these results, all patients harboring *CARD11* mutations did not show optimal responses to the initial 2 cycles of R-CHOP and were classified into the nOR group. However, all these patients achieved and maintained CR at least for 3 y by the early conversion to RB treatment. These results raised the possibility that the negative impact of *CARD11* mutations observed under R-CHOP treatment might be canceled by RB treatment.

We also assessed whether m7-FLIPI is useful to predict prognosis of our RB-treated FL patients. Although the 3-y PFS rate tended to be higher in the m7-FLIPI low group than in the m7-FLIPI high group, this difference was not significant. Also, whereas m7-FLIPI was reported to be able to predict POD24 in R-CHOP-treated FL patients, POD24 was observed regardless of m7-FLIPI risk group in our RB-treated cases. It must be noted that the results reported in this study may lack statistical power due to the small number of cases. In accordance with our results, however, m7-FLIPI had no prognostic value in RB-treated or GB (G + B)-treated FL patients, as reported in a randomized phase III (GALLIUM) trial.^{3,40} Together, these results suggested that m7-FLIPI may not be an accurate prognostic factor in FL patients treated with B-based regimens.

A GEP score based on the expression of 23 genes was initially established to predict clinical outcomes in FL patients,¹⁹ and based on the 23-gene expression panel, it was possible to identify 2 main clusters associated with favorable or poor outcome in the subsequent study.²⁰ However, these studies included only a few patients treated with RB. Subsequently, this model was shown to have no prognostic value in the RB-treated or GB-treated cohort in the GALLIUM study.⁴¹ In accordance with this result, we found that the 3-y PFS rates did not differ between the patients in cluster 1 and cluster 2. However, cluster 2 patients tended to have an inferior 3-y PFS rate compared with cluster 1 patients. Considering the small number of patients in this study, further studies are needed to draw a definite conclusion as to the efficacy of this model in predicting the prognosis of B-treated FL cases.

Several lines of evidence indicated that FL cells depend on the interactions with non-malignant cells that constitute the TME for their growth and survival.^{1,42} Particularly, because of the indolent feature of FL cells, the prognosis of FL is substantially affected by the TME, which consists of various types of T lymphocytes (CTLs, Tregs, and so on), B lymphocytes, and TAMs. These cells act as positive or negative regulators of the immune response in FL, thereby influencing the clinical outcomes in this disease. At first, Dave and colleagues showed that FL patients with high levels of immune infiltration in tumoral tissues had a better prognosis compared with those with low immune infiltration.⁴³ However, this study was conducted before the R era, including some patients who initially received a watch-and-wait approach. Another study showed that a cytotoxic effector T-cell signature based on a signature containing

6 genes (*GZMA*, *GZMB*, *PRF1*, *IFN- γ* , *EOMES*, and *CD8A*) could be a prognostic factor, in which the “inflamed” subset (effector T-cell^{high}) showed better PFS than the “uninflamed” subset (effector T-cell^{low}).⁴⁴ More recently, Tobin and co-workers analyzed the immune infiltration profile in FL cases with or without POD24, and observed that a low expression of immune effectors (*TNF α* , *CD4*), checkpoints (programmed death-ligand 2 [*PD-L2*]), or macrophage markers (*CD68*), were associated with POD24. Among them, *PD-L2* was the most sensitive marker in identifying patients with a poor prognosis.¹¹ However, most of the patients enrolled in these studies received R-CHOP/R-CVP.

To elucidate the roles of the immune microenvironment in RB-treated FL patients, we applied a customized pan-cancer immune-profiling panel consisting of 800 genes to the RB-treated cases in the nOR group. As a result, we found that CD8⁺ T-cell markers such as *CD8A*, *CD8B*, *FLT3LG*, *GZMM*, and *GZMK*, were downregulated in the POD24 group, while markers for NK/T cells and immune checkpoint molecules were almost equivalently expressed in cases with or without POD24. Among the genes downregulated in the POD24 group, *GZMM* and *GZMK*, which are commonly expressed in CTLs and NK cells, have pro-apoptotic activities on tumor cells.⁴⁵ A low expression of *GZMM* and *GZMK* in tumor tissues has been associated with an unfavorable prognosis in cutaneous melanoma,⁴⁶ and *GZMK* was also found to be downregulated in the process of FL transformation.⁴⁷ Together, these results suggested that anti-FL immune responses may be weakened in RB-treated FL patients undergoing POD24. However, future studies using high-throughput technologies, such as single-cell transcriptome sequencing, multicolor immunohistochemistry, and imaging mass cytometry are needed to determine which T-cell subpopulations indeed express each cytotoxic molecule.

In the presented study, some genes related to differentiation (*EOMES*,^{31,32} *TBX-21*³³) or migration (*CXCR3*^{34,35}) of CD8⁺ T cells were also significantly downregulated in the POD24 group. Unexpectedly, *CCR4* was also downregulated in the POD24 group. This result seems to be somewhat unreasonable because targeting therapies against *CCR4* were expected to have great potential in cancer immunotherapies through depletion of Tregs.⁴⁸ However, using single-cell transcriptome sequencing, a recent study has reported that the expression of *CCR4* was positively correlated with CTLs signature and a good prognosis in patients with nasopharyngeal carcinoma.⁴⁹ Collectively, we further classified RB-treated cases into infil^{high} and infil^{low} clusters using the 10 manually selected genes. POD24 was observed in 8/20 (40%) cases in the infil^{low} cluster, while none of infil^{high} cases underwent POD24 ($P = .0084$). Furthermore, we generated the IIS using principal component analysis based on the 10 genes. The 3-y PFS rate was significantly lower in the IIS^{low} group than in the IIS^{high} group ($P = .0237$). These results suggested that our model would be useful for predicting clinical outcomes including POD24 in RB-treated FL patients. Although it has already been shown that an increased number of CD8⁺ T cells in neoplastic follicles of FL was associated with a favorable prognosis,⁵⁰ CD8⁺ T cells present in neoplastic follicles are functionally heterogeneous and

include some exhausted T cells with inhibitory receptors (ie, PD-1, LAG3).⁵¹ So, to identify truly functional CTLs against FL cells among CD8⁺ T cells by immunohistochemistry in daily practice, we should identify several surface markers and utilize them in combination. Furthermore, it should be noted that our RB-treated patients constituted a unique population, namely those who received RB after 2 cycles of R-CHOP. Therefore, future studies are required to determine whether our results are applicable to de novo FL patients treated with a B-based regimen as the 1st-line treatment using larger prospective cohorts.

To clarify molecular mechanisms underlying the difference in infil^{low} and infil^{high} immune profiles, we compared the frequency of mutations in both clusters. However, the frequencies of mutations were roughly the same between infil^{low} and infil^{high} clusters in most genes, especially those that regulate the TME such as *CREBBP*, *EZH2*, and *TNFRSF14*. These results raised the possibility that epigenetic regulation might be different between the 2 clusters. Of importance, the only significant clinical parameter related to the IIS^{low} group was lymphopenia, which we had previously identified as a poor prognostic marker for RB-treated patients.²¹ These results suggested that lymphopenia at diagnosis may reflect reduced T-cell-mediated immune reactions in the TME and that it may be possible to substitute this for the immune profiling utilized in this study.

In conclusion, we here found that the expression of CD8⁺ T-cell markers was significantly lower in RB-treated patients with POD24 than those without POD24. Furthermore, FL cases were classified into IIS^{low} and IIS^{high} groups based on the expression of T-cell-associated genes, which was useful to predict the prognosis of RB-treated FL patients.

ACKNOWLEDGMENTS

The authors thank the patients who participated in the study, their supporters, the investigators, and clinical research staff from the study centers.

CONFLICT OF INTEREST

IM has received research funding from Chugai and Eisai Pharmaceuticals. SR has received payment for lectures from Chugai Pharmaceuticals. No other potential conflicts of interest were reported.

ORCID

Shinya Rai  <https://orcid.org/0000-0003-3929-9751>

Kazuko Sakai  <https://orcid.org/0000-0003-1822-2720>

Mitsuhiro Matsuda  <https://orcid.org/0000-0002-4068-166X>

Yasuhiro Taniguchi  <https://orcid.org/0000-0003-0754-7415>

J. Luis Espinoza  <https://orcid.org/0000-0002-1794-6666>

Kazuto Nishio  <https://orcid.org/0000-0002-8275-0846>

Itaru Matsumura  <https://orcid.org/0000-0003-2818-4270>

REFERENCES

- Carbone A, Roulland S, Gloghini A, et al. Follicular lymphoma. *Nat Rev Dis Primers*. 2019;5:83.
- Hiddemann W, Barbui AM, Canales MA, et al. Immunochemotherapy With Obinutuzumab or Rituximab for Previously Untreated Follicular Lymphoma in the GALLIUM Study: Influence of Chemotherapy on Efficacy and Safety. *J Clin Oncol*. 2018;36:2395-2404.
- Marcus R, Seymour JF, Hiddemann W. Obinutuzumab Treatment of Follicular Lymphoma. *N Engl J Med*. 2017;377:2605-2606.
- Federico M, Luminari S, Dondi A, et al. R-CVP versus R-CHOP versus R-FM for the initial treatment of patients with advanced-stage follicular lymphoma: results of the FOLL05 trial conducted by the Fondazione Italiana Linfomi. *J Clin Oncol*. 2013;31:1506-1513.
- Luminari S, Ferrari A, Manni M, et al. Long-Term Results of the FOLL05 Trial Comparing R-CVP Versus R-CHOP Versus R-FM for the Initial Treatment of Patients With Advanced-Stage Symptomatic Follicular Lymphoma. *J Clin Oncol*. 2018;36:689-696.
- Rummel MJ, Niederle N, Maschmeyer G, et al. Bendamustine plus rituximab versus CHOP plus rituximab as first-line treatment for patients with indolent and mantle-cell lymphomas: an open-label, multicentre, randomised, phase 3 non-inferiority trial. *Lancet*. 2013;381:1203-1210.
- Flinn IW, van der Jagt R, Kahl BS, et al. Randomized trial of bendamustine-rituximab or R-CHOP/R-CVP in first-line treatment of indolent NHL or MCL: the BRIGHT study. *Blood*. 2014;123:2944-2952.
- Flinn IW, van der Jagt R, Kahl B, et al. First-Line Treatment of Patients With Indolent Non-Hodgkin Lymphoma or Mantle-Cell Lymphoma With Bendamustine Plus Rituximab Versus R-CHOP or R-CVP: Results of the BRIGHT 5-Year Follow-Up Study. *J Clin Oncol*. 2019;37:984-991.
- Sarkozy C, Maurer MJ, Link BK, et al. Cause of death in follicular lymphoma in the first decade of the rituximab era: A pooled analysis of French and US Cohorts. *J Clin Oncol*. 2019;37:144-152.
- Casulo C, Byrtek M, Dawson KL, et al. Early Relapse of Follicular Lymphoma After Rituximab Plus Cyclophosphamide, Doxorubicin, Vincristine, and Prednisone Defines Patients at High Risk for Death: An Analysis From the National LymphoCare Study. *J Clin Oncol*. 2015;33:2516-2522.
- Tobin JWD, Keane C, Gunawardana J, et al. Progression of Disease Within 24 Months in Follicular Lymphoma Is Associated With Reduced Intratumoral Immune Infiltration. *J Clin Oncol*. 2019;37:3300-3309.
- Seymour JF, Marcus R, Davies A, et al. Association of early disease progression and very poor survival in the GALLIUM study in follicular lymphoma: benefit of obinutuzumab in reducing the rate of early progression. *Haematologica*. 2019;104:1202-1208.
- Solal-Célgny P, Roy P, Colombat P, et al. Follicular lymphoma international prognostic index. *Blood*. 2004;104:1258-1265.
- Federico M, Bellei M, Marcheselli L, et al. Follicular lymphoma international prognostic index 2: a new prognostic index for follicular lymphoma developed by the international follicular lymphoma prognostic factor project. *J Clin Oncol*. 2009;27:4555-4562.
- Bachy E, Maurer MJ, Habermann TM, et al. A simplified scoring system in de novo follicular lymphoma treated initially with immunochemotherapy. *Blood*. 2018;132:49-58.
- Mir F, Mattiello F, Grigg A, et al. Follicular Lymphoma Evaluation Index (FLEX): A new clinical prognostic model that is superior to existing risk scores for predicting progression-free survival and early treatment failure after frontline immunochemotherapy. *Am J Hematol*. 2020;95:1503-1510.
- Pastore A, Jurinovic V, Kridel R, et al. Integration of gene mutations in risk prognostication for patients receiving first-line immunochemotherapy for follicular lymphoma: a retrospective analysis of a prospective clinical trial and validation in a population-based registry. *Lancet Oncol*. 2015;16:1111-1122.
- Jurinovic V, Kridel R, Staiger AM, et al. Clinicogenetic risk models predict early progression of follicular lymphoma after first-line immunochemotherapy. *Blood*. 2016;128:1112-1120.

19. Huet S, Tesson B, Jais JP, et al. A gene-expression profiling score for prediction of outcome in patients with follicular lymphoma: a retrospective training and validation analysis in three international cohorts. *Lancet Oncol.* 2018;19:549-561.
20. Silva A, Bassim S, Sarkozy C, et al. Convergence of risk prediction models in follicular lymphoma. *Haematologica.* 2019;104:e252-e255.
21. Rai S, Inoue H, Hanamoto H, et al. Low absolute lymphocyte count is a poor prognostic factor for untreated advanced follicular lymphoma treated with rituximab plus bendamustine: results of the prospective phase 2 CONVERT trial. *Int J Hematol.* 2021;114(2):205-216.
22. Cheson BD, Horning SJ, Coiffier B, et al. Report of an international workshop to standardize response criteria for non-Hodgkin's lymphomas. NCI Sponsored International Working Group. *J Clin Oncol.* 1999;17:1244.
23. Sakai K, Tsuboi M, Kenmotsu H, et al. Tumor mutation burden as a biomarker for lung cancer patients treated with pemetrexed and cisplatin (the JIPANG-TR). *Cancer Sci.* 2021;112:388-396.
24. Watatani Y, Sato Y, Miyoshi H, et al. Molecular heterogeneity in peripheral T-cell lymphoma, not otherwise specified revealed by comprehensive genetic profiling. *Leukemia.* 2019;33:2867-2883.
25. Rai S, Tanaka H, Suzuki M, et al. Chlorpromazine eliminates acute myeloid leukemia cells by perturbing subcellular localization of FLT3-ITD and KIT-D816V. *Nat Commun.* 2020;11:4147.
26. Sugio T, Miyawaki K, Kato K, et al. Microenvironmental immune cell signatures dictate clinical outcomes for PTCL-NOS. *Blood Adv.* 2018;2:2242-2252.
27. Huet S, Sujobert P, Salles G. From genetics to the clinic: a translational perspective on follicular lymphoma. *Nat Rev Cancer.* 2018;18:224-239.
28. Morin RD, Mendez-Lago M, Mungall AJ, et al. Frequent mutation of histone-modifying genes in non-Hodgkin lymphoma. *Nature.* 2011;476:298-303.
29. Bouska A, Zhang W, Gong Q, et al. Combined copy number and mutation analysis identifies oncogenic pathways associated with transformation of follicular lymphoma. *Leukemia.* 2017;31:83-91.
30. Okosun J, Bödör C, Wang J, et al. Integrated genomic analysis identifies recurrent mutations and evolution patterns driving the initiation and progression of follicular lymphoma. *Nat Genet.* 2014;46:176-181.
31. Pearce EL, Mullen AC, Martins GA, et al. Control of effector CD8+ T cell function by the transcription factor Eomesodermin. *Science.* 2003;302:1041-1043.
32. Takemoto N, Intlekofer AM, Northrup JT, Wherry EJ, Reiner SL. Cutting Edge: IL-12 inversely regulates T-bet and eomesodermin expression during pathogen-induced CD8+ T cell differentiation. *J Immunol.* 2006;177:7515-7519.
33. Joshi NS, Cui W, Chandele A, et al. Inflammation directs memory precursor and short-lived effector CD8(+) T cell fates via the graded expression of T-bet transcription factor. *Immunity.* 2007;27:281-295.
34. Kohli K, Pillarisetty VG, Kim TS. Key chemokines direct migration of immune cells in solid tumors. *Cancer Gene Ther.* 2021. 10.1038/s41417-021-00303-x
35. Hensbergen PJ, Wijnands PG, Schreurs MW, Scheper RJ, Willemze R, Tensen CP. The CXCR3 targeting chemokine CXCL11 has potent antitumor activity in vivo involving attraction of CD8+ T lymphocytes but not inhibition of angiogenesis. *J Immunother.* 2005;28:343-351.
36. Andor N, Simonds EF, Czerwinski DK, et al. Single-cell RNA-Seq of follicular lymphoma reveals malignant B-cell types and coexpression of T-cell immune checkpoints. *Blood.* 2019;133:1119-1129.
37. Béguelin W, Teater M, Meydan C, et al. Mutant EZH2 Induces a Pre-malignant Lymphoma Niche by Reprogramming the Immune Response. *Cancer Cell.* 2020;37:655-673.
38. Boice M, Salloum D, Mourcin F, et al. Loss of the HVEM Tumor Suppressor in Lymphoma and Restoration by Modified CAR-T Cells. *Cell.* 2016;167:405-418.
39. Devan J, Janikova A, Mraz M. New concepts in follicular lymphoma biology: From BCL2 to epigenetic regulators and non-coding RNAs. *Semin Oncol.* 2018;45:291-302.
40. Jurinovic V, Passerini V, Oestergaard MZ, et al. Evaluation of the m7-FLIPI in Patients with Follicular Lymphoma Treated within the Gallium Trial: EZH2 mutation Status May be a Predictive Marker for Differential Efficacy of Chemotherapy. *Blood.* 2019;134:122.
41. Bolen CR, Hiddemann W, Marcus R, et al. Treatment-dependence of high-risk gene expression signatures in de novo follicular lymphoma. *International Conference on Malignant Lymphoma (ICML), June 18th-22nd, 2019, Abstract 143.*
42. Inoue H, Rai S, Tanaka H, et al. Tumour-immune microenvironment in duodenal-type follicular lymphoma. *Br J Haematol.* 2020;191(2):243-252.
43. Dave SS, Wright G, Tan B, et al. Prediction of survival in follicular lymphoma based on molecular features of tumor-infiltrating immune cells. *N Engl J Med.* 2004;351:2159-2169.
44. Bolen CR, McCord R, Huet S, et al. Mutation load and an effector T-cell gene signature may distinguish immunologically distinct and clinically relevant lymphoma subsets. *Blood Adv.* 2017;1:1884-1890.
45. Voskoboinik I, Whisstock JC, Trapani JA. Perforin and granzymes: function, dysfunction and human pathology. *Nat Rev Immunol.* 2015;15:388-400.
46. Wu X, Wang X, Zhao Y, Li K, Yu B, Zhang J. Granzyme family acts as a predict biomarker in cutaneous melanoma and indicates more benefit from anti-PD-1 immunotherapy. *Int J Med Sci.* 2021;18:1657-1669.
47. de Vos S, Hofmann WK, Grogan TM, et al. Gene expression profile of serial samples of transformed B-cell lymphomas. *Lab Invest.* 2003;83:271-285.
48. Kang S, Xie J, Ma S, Liao W, Zhang J, Luo R. Targeted knock down of CCL22 and CCL17 by siRNA during DC differentiation and maturation affects the recruitment of T subsets. *Immunobiology.* 2010;215:153-162.
49. Li H, Chen X, Zeng W, et al. Radiation-enhanced expression of CCL22 in nasopharyngeal carcinoma is associated with CCR4. *Int J Radiat Oncol Biol Phys.* 2020;108:126-139.
50. Alvaro T, Lejeune M, Salvadó MT, et al. Immunohistochemical patterns of reactive microenvironment are associated with clinical behavior in follicular lymphoma patients. *J Clin Oncol.* 2006;24:5350-5357.
51. Kurachi M. CD8. *Semin Immunopathol.* 2019;41:327-337.

SUPPORTING INFORMATION

Additional supporting information may be found in the online version of the article at the publisher's website.

How to cite this article: Rai S, Inoue H, Sakai K, et al. Decreased expression of T-cell-associated immune markers predicts poor prognosis in patients with follicular lymphoma. *Cancer Sci.* 2022;113:660–673. doi:[10.1111/cas.15224](https://doi.org/10.1111/cas.15224)